

EXCITED LEPTON SEARCH

CELLO Collaboration

H.-J. BEHREND, J. BÜRGER, L. CRIEGEE, H. FENNER, J.H. FIELD, G. FRANKE,
J. FUSTER¹, Y. HOLLER, J. MEYER, V. SCHRÖDER, H. SINDT, U. TIMM, G.G. WINTER,
W. ZIMMERMANN

Deutsches Elektronen-Synchrotron, DESY, D-2000 Hamburg 52, Germany

P.J. BUSSEY, A.J. CAMPBELL, J.B. DANTON, D. HENDRY, G. McCURRACH, J.M. SCARR,
I.O. SKILLICORN, K.M. SMITH

University of Glasgow, Glasgow G12 8QQ, United Kingdom

V. BLOBEL, M. POPPE, H. SPITZER

II. Institut für Experimentalphysik, Universität Hamburg, D-2000 Hamburg 50, Germany

W.-D. APEL, J. ENGLER, G. FLÜGGE, D.C. FRIES, W. FUES², K. GAMERDINGER,
P. GROSSE-WIESMANN, J. HANSMEYER, Th. HENKES, G. HOPP, H. JUNG, J. KNAPP,
M. KRÜGER, H. KÜSTER, H. MÜLLER, K.H. RANITZSCH, H. SCHNEIDER

Kernforschungszentrum Karlsruhe and Universität Karlsruhe, D-7500 Karlsruhe, Germany

W. DE BOER, G. BUSCHHORN, W. CHRISTIANSEN, G. GRINDHAMMER,
B. GUNDERSON, Ch. KIESLING, R. KOTTHAUS, H. KROHA, D. LÜERS, H. OBERLACK,
B. SACK, P. SCHACHT, G. SHOOSHTARI, W. WIEDENMANN

Max-Planck-Institut für Physik und Astrophysik, D-8000 Munich 40, Germany

A. CORDIER, M. DAVIER, D. FOURNIER, M. GAILLARD, J.F. GRIVAZ, J. HAISSINSKI,
P. JANOT, V. JOURNÉ, F. LE DIBERDER, E. ROS³, A. SPADAFORA, J.-J. VEILLET

Laboratoire de l'Accélérateur Linéaire, F-91405 Orsay Cedex, France

B. FATAH, R. GEORGE, M. GOLDBERG, O. HAMON, F. KAPUSTA, F. KOVACS, R. PAIN,
L. POGGIOLI, M. RIVOAL

Laboratoire de Physique Nucléaire et Hautes Energies, Université de Paris, F-75231 Paris Cedex 05, France

G. D'AGOSTINI, M. GASPERO, B. STELLA

University of Rome and INFN, I-00185 Rome, Italy

R. ALEKSAN, G. COZZIKA, Y. DUCROS, P. JARRY, Y. LAVAGNE, F. OULD SAADA,
J. PAMELA, F. PIERRE, J. ZACEK⁴

Centre d'Etudes Nucléaires, Saclay, F-91191 Gif-sur-Yvette Cedex, France

G. ALEXANDER, G. BELLA, Y. GNAT and J. GRUNHAUS

Tel Aviv University, Ramat Aviv, Tel Aviv 69978, Israel

Received 8 January 1986

Using the CELLO detector at PETRA a search has been made for excited leptons by studying e^+e^- interactions which yield $\ell^+\ell^-\gamma\gamma$, $\ell^+\ell^-\gamma$ and $\gamma\gamma$ final states, where $\ell = e, \mu$ or τ . Good agreement with QED is observed and new limits are set on e^* , μ^* , and τ^* production.

Excited lepton states are expected in models in which leptons are composite particles [1]. In e^+e^- collisions, such excited states could be produced either in pairs due to the normal gauge couplings, or singly when a radiative transition occurs between a normal and an excited lepton. Also, the existence of an excited electron would modify the photon pair production cross section by introducing an additional propagator. For the $\ell^*\ell\gamma$ coupling needed in the latter two cases we use the following gauge invariant effective lagrangian [2]:

$$L_{\text{eff}} = (\lambda\theta/2M_{\ell^*})\bar{\ell}^*\sigma_{\mu\nu}\ell F^{\mu\nu} + \text{h.c.}, \quad (1)$$

where λ is a dimensionless free parameter which characterizes the strength of the $\ell^*\ell\gamma$ coupling, and M_{ℓ^*} is the mass of the excited lepton. An alternative parametrization of L_{eff} consists in replacing M_{ℓ^*} in (1) by the compositeness scale Λ . To avoid this ambiguity, the results of our analysis are expressed in terms of (λ/M_{ℓ^*}) rather than in terms of λ .

Since the compositeness scale Λ is expected to be in the TeV range or above [3] one can safely neglect any form factor effect when considering an excited lepton mass in the PETRA energy range. More general expressions for the effective lagrangian could be considered. For instance Renard [4] and Hagiwara et al. [5] introduce an additional factor $(a - b\gamma_5)$ motivated by chiral symmetry arguments. For the sake of clarity we use the simplest form of L_{eff} . Nevertheless our limits on (λ/M_{ℓ^*}) would remain essentially unaffected by such a modification if the convention $|a|^2 + |b|^2 = 1$ is used.

We have searched for evidence for excited leptons

¹ On leave of absence from Instituto de Fisica Corpuscular, Universidad de Valencia, Valencia, Spain.

² Present address: SCS, D-2000 Hamburg, Germany.

³ Present address: Universidad Autónoma de Madrid, Canto Blanco, Madrid 34, Spain.

⁴ On leave of absence from Nuclear Center, Charles University, CS-180 00 Prague 8, Czechoslovakia.

in the following three processes:

(1) pair production of ℓ^*

$$ee \rightarrow \ell^*\ell^* \rightarrow \ell\ell\gamma\gamma, \quad \ell = e, \mu, \tau,$$

(2) single production of ℓ^*

$$ee \rightarrow \ell^*\ell \rightarrow \ell\ell\gamma, \quad \ell = e, \mu, \tau,$$

(3) photon pair production

$$ee \rightarrow \gamma\gamma.$$

Data collection and detector properties. The data were collected with the CELLO detector operating at the PETRA e^+e^- collider at DESY. The centre-of-mass energy varied from 33 to 46.8 GeV. The total integrated luminosity is about 30 pb^{-1} . Table 1 summarizes the luminosities used for the various reactions, together with the number of events observed in each case within the cuts described below.

The CELLO detector has been described in detail elsewhere [6]. The main features of the apparatus used in this analysis are its good angular resolution, its large and uniform coverage for detection of charged particles and photons, and its ability to identify electrons, muons and tau-decays. For this analysis we have only considered charged particles and photons in

Table 1
Data sample for the various analyzed processes.

Reaction	Integrated luminosity (pb^{-1})	\sqrt{s} (GeV)	Number of events
$ee \rightarrow e\theta\gamma$	29.2	33.0–46.8	239
$ee \rightarrow ee\gamma\gamma$	29.2	33.0–46.8	2
$ee \rightarrow e\gamma(e)$	14.0	44.0–46.8	410
$ee \rightarrow \mu\mu\gamma$	32.6	33.0–46.8	26
$ee \rightarrow \mu\mu\gamma\gamma$	32.6	33.0–46.8	2
$ee \rightarrow \tau\tau\gamma$	21.6	40.0–46.8	8
$ee \rightarrow \tau\tau\gamma\gamma$	21.6	40.0–46.8	1
$ee \rightarrow \gamma\gamma$	28.9	33.0–46.8	2533

the polar angle range $|\cos\theta| < 0.85$ which is covered by the central calorimeter. In this region the angular resolutions for charged particles are $\sigma_\theta = 3 \text{ mrad} \sin^2\theta$ and $\sigma_\phi = 2 \text{ mrad}$ and the corresponding photon angular resolutions are $\sigma_\theta = 10 \text{ mrad}$ and $\sigma_\phi = 6 \text{ mrad}$.

For reactions with 3- and 4-body final states, the kinematics can be precisely reconstructed from accurate angular measurements. With the angular resolutions quoted above, a typical resolution of

$$\sigma(M_{\ell\gamma}) \cong 300 \text{ MeV} \quad (\ell = e, \mu) \quad (2)$$

is achieved [7] for the lepton–photon invariant mass.

Event selection and analysis.

(1) *Pair production.* For the reactions $ee \rightarrow ee\gamma\gamma$ and $ee \rightarrow \mu\mu\gamma\gamma$ we require the lepton momentum to be larger than $0.05E_b$, where E_b is the beam energy. The more energetic photon is required to have an energy larger than $0.4E_b$ and the other to have an energy larger than $0.1E_b$. The opening angle for each pair of particles is required to be larger than 10° .

Electrons and muons are identified by their characteristic behaviour in a finely segmented lead–liquid-argon calorimeter and, in the case of muons, by their ability to penetrate a 80 cm thick iron filter, beyond which large drift chambers are located. Two $ee\gamma\gamma$ and two $\mu\mu\gamma\gamma$ events are observed.

Pair-produced excited leptons would show up as events with two lepton–photon pairs of equal mass. Fig. 1 shows the lepton–photon mass correlations obtained from our data sample. Within the mass resolution (2), no event satisfying the equal mass hypothesis is observed.

For the reaction $ee \rightarrow \tau\tau\gamma\gamma$ we consider only the two-prong topology. We require the sum of the momenta of the charged particles to be larger than $0.1E_b$ and two isolated photons with the same energy criteria as above. To avoid confusion with photons originating from τ -decays, the mass of each isolated photon with each of the two charged particles is required to be greater than 1.5 GeV. The tau-decays are then identified with the help of the calorimeter and the muon chambers [8]. One event is found within these cuts. Owing to the unobserved neutrinos in the tau-decays no precise $\tau\gamma$ invariant mass reconstruction is possible. Therefore this event has been kept as a candidate.

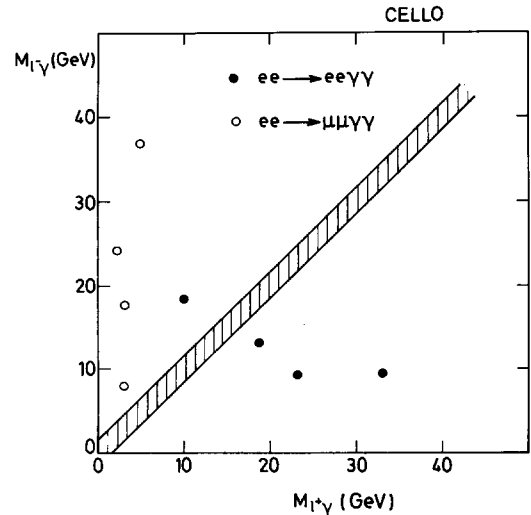


Fig. 1. The lepton–photon mass correlations in the reactions $ee \rightarrow ee\gamma\gamma$ and $ee \rightarrow \mu\mu\gamma\gamma$ (2 entries per event). Pair produced excited leptons would appear in the hatched region.

(2) *Single production.* For single production of ℓ^* , through $ee \rightarrow \ell\ell^* \rightarrow \ell\ell\gamma$, we consider two different final state topologies. In the first one, the two final state leptons and the decay photon are all observed in the central detector. A second topology, well suited to the study of e^* production, is provided by the “virtual Compton scattering” configuration, $ee \rightarrow e\gamma(e)$ [4,5,9]. Here only the decay products of the e^* are observed. The other electron stays close to the beam direction and remains undetected.

In the first case the event selection was carried out with the same criteria as for pair production, except that we require only one photon with an energy larger than $0.4E_b$ [7]. To reduce the contributions from radiative events arising from higher order QED processes, the lepton–photon and lepton–lepton invariant masses are required to be larger than 10% of the centre-of-mass energy.

We observe 239 $ee\gamma$ events, 26 $\mu\mu\gamma$ events and 8 $\tau\tau\gamma$ events, where Monte Carlo calculations of radiative QED processes [10] predict respectively 230, 25 and 11 events.

Since the reactions $ee \rightarrow ee\gamma$ and $ee \rightarrow \mu\mu\gamma$ are kinematically overconstrained it is possible to take into account the emission of a photon along the beam direction. Performing the kinematical reconstruction mentioned previously, we obtain the lepton–photon

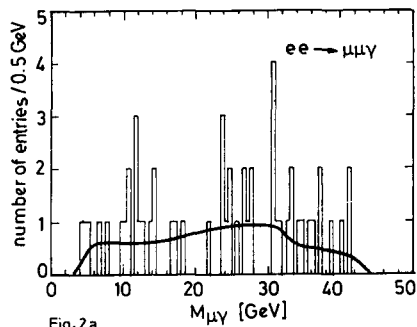


Fig. 2a

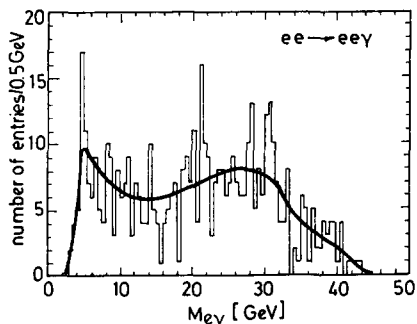


Fig. 2. The lepton-photon mass distributions in the processes $ee \rightarrow ee\gamma$ and $ee \rightarrow \mu\mu\gamma$ (2 entries per event). The solid line corresponds to the QED expectation.

invariant mass distributions shown in fig. 2. No significant narrow structure is observed.

Here again, in the reaction $ee \rightarrow \tau\tau\gamma$, due to the unobserved neutrinos in the tau-decays, the $\tau\gamma$ invariant mass distribution has not been considered.

For the reaction $ee \rightarrow e\gamma(e)$ we require an electron-photon pair coplanar with the beam direction ($\Delta\Phi > 177^\circ$) with a total energy greater than $0.85E_b$. 410 events are observed, where a Monte Carlo calculation predicts 420 events for the $ee \rightarrow e\gamma(e)$ process, taking into account possible radiation by the incoming electron which is scattered at large angle.

For these events, the unobserved electron may be assumed to be scattered along the beam direction: since in 80% of them the polar angle of this electron is less than 10 mrad, the error thus introduced is comparable to the one made in the measurement of the directions of the observed electron and photon. Fig. 3 shows the invariant mass distribution which has been obtained. It agrees with the QED expectation and does not show any significant narrow structure.

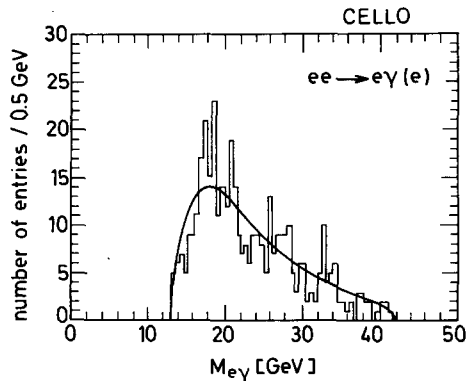


Fig. 3. The electron-photon mass distribution in the "virtual Compton scattering" configuration $ee \rightarrow e\gamma(e)$ (1 entry per event). The solid line corresponds to the QED expectation.

(3) *Photon pair production.* For the reaction $ee \rightarrow \gamma\gamma$ we observe 2533 events. Details of the analysis can be found elsewhere [11]. The data taken at the highest centre-of-mass energy have not been presented so far. Detection efficiencies are determined by studying the Bhabha scattering events which are observed with both the liquid-argon calorimeter and the central tracking device.

With the luminosity deduced from the large angle Bhabha scattering process the measured cross sections are $\sigma_{\text{exp}}/\sigma_{\text{QED}} = 0.96 \pm 0.04, 0.96 \pm 0.06$ and 0.98 ± 0.05 at centre-of-mass energies of 43.2 GeV, 42.4 GeV and 44.2 GeV respectively. The QED expectations are obtained using a Monte Carlo calculation which takes into account corrections up to the order α^3 [22]. The polar angle distribution for the three different centre-of-mass energies are shown in fig. 4. All are in agreement with the QED expectation.

Results and discussion. The different cross section for pair production of fermions of mass M via one-photon annihilation is:

$$\frac{d\sigma}{d\Omega} = \frac{\alpha^2}{4s} \beta [1 + \cos^2\theta + (1 - \beta^2) \sin^2\theta], \quad (3)$$

where $s = 4E_b^2$ and $\beta^2 = 1 - 4M^2/s$.

Using this formula and taking into account initial state radiative corrections, we derive 95% CL lower limits for the masses of e^* , μ^* and τ^* of 23, 23 and 22.7 GeV respectively.

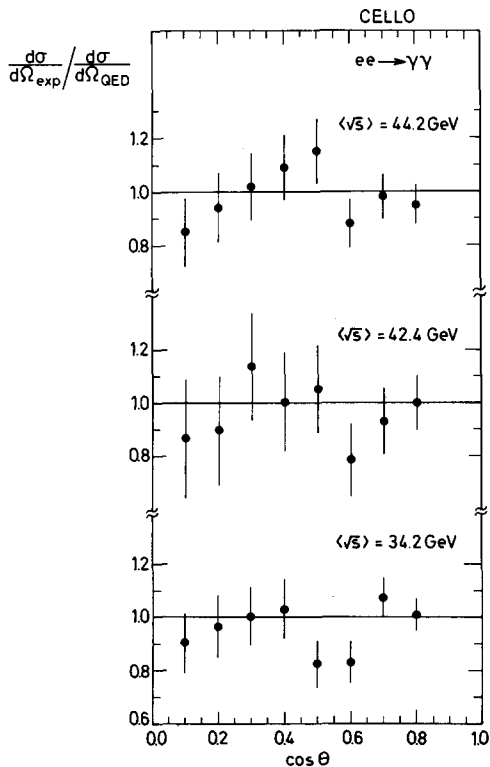


Fig. 4. The differential cross section for the reaction $ee \rightarrow \gamma\gamma$ normalized to the QED prediction, for three energy ranges.

To set upper limits on the coupling strength which enters in the effective lagrangian (1) the following formulae used are for the differential cross sections⁺¹ [4]:

$$\frac{d\sigma}{dt} = -\frac{2\pi\alpha^2\lambda^2}{M_{e^*}^2 s^2} \left(\frac{t^2 + (t - M_{e^*}^2)^2}{s} + \frac{s^2 + (s - M_{e^*}^2)^2}{t} + m_e^2 \frac{2M_{e^*}^4}{t^2} \right), \quad (4)$$

for single e^* production, and

$$\frac{d\sigma}{dt} = \frac{2\pi\alpha^2\lambda^2}{M_{Q^*}^2 s^2} \left(\frac{M_{Q^*}^2(s - M_{Q^*}^2) + 2tu}{s} \right), \quad (5)$$

⁺¹ As stated previously, formulae (4), (5), (6) and (7), which follow, are not modified by the insertion of a $(a - b\gamma_5)$ factor in the expression of the effective lagrangian (1). The inclusion of such a factor only leads to a slight change of our acceptance for the reaction $ee \rightarrow \ell\ell^* \rightarrow \ell\ell\gamma$.

for single μ^* and τ^* production, where s , t and u are the usual Mandelstam variables.

In the reactions $ee \rightarrow e\gamma$ and $ee \rightarrow \mu\mu\gamma$ we derive 95% CL upper limits for $(\lambda/M_{e^*})^2$ from the invariant mass distributions of fig. 2, after a bin-to-bin subtraction of the known QED contribution⁺². In the reaction $ee \rightarrow \tau\tau\gamma$ upper limits are determined from the total number of observed events only.

To derive upper limits on $(\lambda/M_{e^*})^2$ from the virtual Compton scattering we use the maximum likelihood method considering only the shape of the invariant mass distribution. We do not consider the photon angular distribution in the electron-photon centre-of-mass frame, since it depends⁺³ on the actual values chosen for the parameters a and b discussed previously according to

$$\frac{d\sigma}{d\cos\theta} (e^{*\pm} \rightarrow e^\pm\gamma) \sim 1 - 2 \text{Re}(ab^*) \cos\theta, \quad (4')$$

where θ is the polar angle in the e^{*+} (e^{*-}) centre-of-mass frame of the final state photon with respect to the positron (electron) beam direction [5].

Unlike for the production of real ℓ^* states discussed above, the sensitivity on M_{e^*} of the reaction $ee \rightarrow \gamma\gamma$ extends beyond the centre-of-mass energy. At the lowest order in λ , the e^* propagator modifies the differential QED cross section of this reaction in the following way [2]:

$$\frac{d\sigma}{d\Omega} \Big|_{\Lambda_+} = \frac{d\sigma^{\text{QED}}}{d\Omega} [1 + (s^4/2\Lambda_+^4) \sin^2\theta H(\cos^2\theta)], \quad (6)$$

where the conventionally used Λ_+ cut off parameter is related to λ and M_{e^*} by $\lambda = M_{e^*}^2/\Lambda_+^2$ and where the function $H(\cos^2\theta)$ is given by

$$H(\cos^2\theta) = [2M_{e^*}^2/(2M_{e^*}^2 + s)]^2 \times \{1 + [(1 - \cos^2\theta)/(1 + \cos^2\theta)]s/2M_{e^*}^2\} \times \{1 - \cos^2\theta [s/(2M_{e^*}^2 + s)]^2\}^{-1}. \quad (7)$$

For large values of $M_{e^*}^2$ ($M_{e^*}^2 \gg s$) the function $H(\cos^2\theta)$ tends to unity. In this case a fit to the polar angle distribution shown in fig. 4 gives a 95% CL lower limit of 84 GeV for Λ_+ .

⁺² A detailed comparison of our $ee\gamma$ and $\mu\mu\gamma$ data with QED can be found in ref. [7].

⁺³ This dependence has no effect on the total cross section because our selection criteria are the same for both the final state electron and photon.

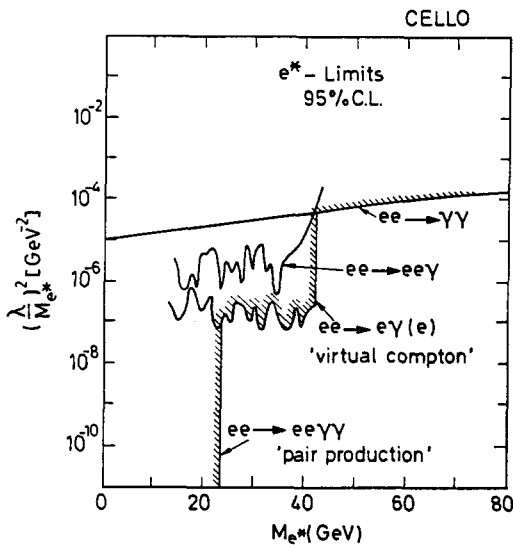


Fig. 5. The 95% CL upper limits for $(\lambda/M_{e^*})^2$ as a function of M_{e^*} as derived from the reactions $ee \rightarrow ee\gamma\gamma$, $ee \rightarrow ee\gamma$, $ee \rightarrow e\gamma(e)$ and $ee \rightarrow \gamma\gamma$.

The limits derived from the various reactions which we analyzed are summarized in figs. 5 and 6.

e^* masses lower than 23 GeV are excluded by our study of the reaction $ee \rightarrow ee\gamma\gamma$. For masses from 23 GeV up to 42 GeV the most stringent limits on

$(\lambda/M_{e^*})^2$ come from the virtual Compton scattering and are typically of the order of 10^{-7} GeV^{-2} . The structure displayed by the curves merely reflects the statistical fluctuations in the lepton-photon invariant mass distributions. Above $M_{e^*} = 42$ GeV the reaction $ee \rightarrow \gamma\gamma$ provides an upper bound on $(\lambda/M_{e^*})^2$ of the order of 10^{-4} GeV^{-2} , corresponding to the lower limit of 84 GeV derived for the Λ_+ parameter. Using the complete formula (6) it can be seen that the limit saturates at 10^{-5} GeV^{-2} for small M_{e^*} values.

For μ^* production outside the region excluded by pair production, limits of the order of 10^{-5} GeV^{-2} on $(\lambda/M_{\mu^*})^2$ are achieved. The limits on τ^* -production are less stringent because of the lower detection efficiency and because we do not consider the invariant mass distribution. The latter fact explains moreover the smoothness of the τ^* -limit in fig. 6.

For e^* and μ^* , our analysis^{†4} which uses the highest PETRA energies improves significantly the limits previously published by the PLUTO, MAC, JADE, TASSO and MARK-J Collaborations [13]. For the τ^* no limit has been published so far.

Conclusion. We have observed the reactions $ee \rightarrow \ell\ell\gamma(\gamma)$, where $\ell = e, \mu$ or τ and the reaction $ee \rightarrow \gamma\gamma$ and have obtained good agreement with the expectations from known QED processes. No indication of an excited electron, muon or tau is observed up to the highest PETRA energy of 46.8 GeV.

Lower limits at 95% CL of 23.0 GeV for the e^* and μ^* masses and 22.7 GeV for the τ^* mass are derived from the non observation of pair production. Limits are put on the coupling strength for the $\ell^* \rightarrow \ell\gamma$ transition for a hypothetical excited lepton up to masses of about 42 GeV from the non observation of single production. A lower limit of 84 GeV is set for the Λ_+ cut-off parameter for the reaction $ee \rightarrow \gamma\gamma$.

We gratefully acknowledge the outstanding efforts of the PETRA machine group which made possible these measurements. We are indebted to the DESY

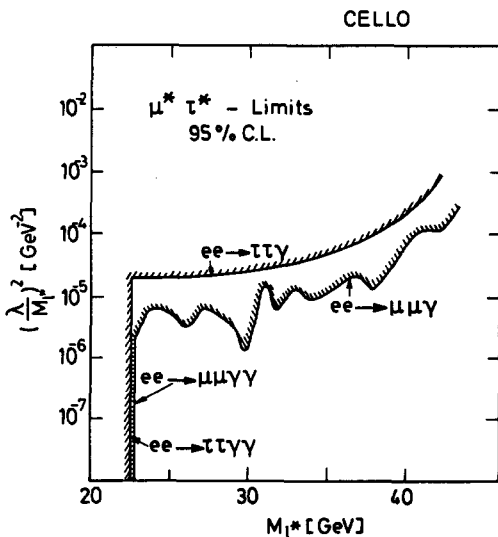


Fig. 6. The 95% CL upper limits for $(\lambda/M_{\ell^*})^2$ as a function of M_{ℓ^*} ($\ell = \mu, \tau$) as derived from the reactions $ee \rightarrow \ell\ell\gamma\gamma$ and $ee \rightarrow \ell\ell\gamma$.

^{†4} Limits on a possible electron or muon substructure can also be derived from $(g-2)$ measurements. However, such limits cannot be compared to ours in a straightforward way because they involve two parameters (M_{ℓ^*} and the compositeness scale Λ , see refs. [14-17]), and because they depend strongly on the type of couplings used at the effective vertices, see refs. [15,17].

computer center for excellent support during the experiment. We acknowledge the invaluable effort of the many engineers and technicians from the collaborating institutions in the construction and maintenance of the apparatus, in particular the operation of the magnet system by M. Clausen, P. Röpnack and the cryogenics group. The visiting groups wish to thank the DESY directorate for the support and kind hospitality extended to them. Special thanks go to Dr. A. Courau, Dr. F.M. Renard and Dr. D. Zeppenfeld for very helpful discussions.

This work was partly supported by the Bundesministerium für Forschung und Technologie (Germany), by the Commissariat à l'Energie Atomique and the Institut National de Physique Nucléaire et de Physique des Particules (France), by the Science and Engineering Research Council (UK), and by the Israeli Ministry of Science and Development.

References

- [1] H. Terazawa et al., Phys. Lett. 112B (1982) 387.
- [2] F.E. Low, Phys. Rev. Lett. 14 (1965) 238;
A. Litke, Thesis Harvard (1970), unpublished.
- [3] E. Eichten et al., Phys. Rev. Lett. 50 (1983) 811.
- [4] F.M. Renard, Z. Phys. C14 (1982) 209.
- [5] K. Hagiwara et al., DESY 85-025 (1985).
- [6] CELLO Collab., H.-J. Behrend et al., Phys. Scr. 23 (1981) 610.
- [7] CELLO Collab., H.-J. Behrend et al., Phys. Lett. 158B (1985) 536.
- [8] CELLO Collab., H.-J. Behrend et al., Phys. Lett. 114B (1982) 282.
- [9] A. Courau and P. Kessler, LAL/85-01 (1985);
J.H. Kühn et al., CERN-TH. 4131/85 (1985).
- [10] F. Berends and R. Kleiss, Nucl. Phys. B177 (1981) 237;
B228 (1983) 537;
F. Berends, R. Kleiss and S. Jadach, Nucl. Phys. B202 (1982) 63.
- [11] CELLO Collab., H.-J. Behrend et al., Phys. Lett. 123B (1983) 127; 140B (1984) 130.
- [12] F. Berends and R. Kleiss, Nucl. Phys. B186 (1981) 22.
- [13] PLUTO Collab., Ch. Berger et al., Phys. Lett. 94B (1980) 87;
MAC Collab., W.T. Ford et al., Phys. Rev. Lett. 51 (1983) 257;
JADE Collab., W. Bartel et al., Z. Phys. C19 (1983) 197;
C24 (1984) 223;
TASSO Collab., M. Althoff et al., Z. Phys. C26 (1984) 337;
MARK-J Collab., B. Adeva et al., Phys. Lett. 152B (1985) 439.
- [14] H. Pietschmann and H. Stremnitzer, Phys. Lett. 37B (1971) 312.
- [15] F.M. Renard, Phys. Lett. 116B (1982) 264.
- [16] F. Cesi, Università di Roma "La Sapienza" preprint n. 432 (1985).
- [17] S. Narison, Phys. Lett. 167B (1986) 214.